Analysis of Outer Race Bearing Damage by Calculation of Sound Signal Frequency Based on the FFT Method

Iradiratu Diah Prahmana Karyatanti[1,*], Ananda Noersena[1], Firsyaldo Rizky Purnomo[1], Rafli Setiawan Zulkifli[1], Ardik Wijayanto[2]

[1]Department of Electrical Engineering, Faculty of Engineering and Marine Science, Hang Tuah University, Surabaya, Indonesia

[2]Department of Electronic Engineering, Electronic Engineering Polytechnic Institute of Surabaya, Surabaya, Indonesia

Received 05 February 2022; received in revised form 16 July 2022; accepted 17 July 2022

DOI: https://doi.org/10.46604/ijeti.2022.9411

Abstract

This study aims to identify the outer race bearing needed to protect an induction motor from severe damage. Faults are diagnosed using a non-invasive technique through the sound signal from an induction motor. The diagnosis aims to assess the damage to the bearings on the fan or main shaft. Moreover, this study discusses the type of damage, loading variations, and the diagnostic accuracy with the damage to the outer race bearing placed on the fan or main shaft rotor. The disturbance detection approach is used to analyze the sound spectrum to identify the harmonic components near the disturbance frequency. The damage frequency characteristics are also calculated to determine the sound spectrum peak value. The results show that the detection is slightly affected by the damage severity and the incorrect placement of the bearings on the rotor shaft. The lowest detection accuracy in testing the outer race bearing damage on the fan shaft is 91.66%. However, the accuracy percentage is 100% with the outer race bearing damage on the main shaft.

Keywords: bearing, sound, frequencies, FFT

1. Introduction

The electric machine widely used in industries is the induction motor, a vital driving tool whose reliability should be maintained for efficient operations [1]. Induction motors have high efficiency, simple construction, low price, and easy maintenance [2]. However, the motors do not operate normally continuously because they have an aging period due to long-term use [3]. Bearings and eccentricity may suffer mechanical damage and the stator and rotor may sufferer electrical damage [4]. The Electric Power Research Institute (EPRI) and the Institute of Electrical and Electronics Engineers Industry Applications Society (IEEE-IAS) found that motor bearings suffered the biggest damage [5]. Bearings limit the relative motion of two or more machine components by being moved in the desired direction [6]. Damage to bearings causes vibration, overheating, and noise [7], while abnormal use of an induction motor results in financial losses, damages to other motor parts, or workplace accidents. These adverse effects are overcome by monitoring the bearing condition as periodic maintenance information using diagnosis by invasive and non-invasive techniques [8].

Motor current signature analysis (MCSA) is an invasive technique that requires expensive equipment and data collection through direct contact with motor parts [9]. However, MCSA applies to all motors, including pumps operated on wet media [10]. The technique is also recommended because the detection results are more accurate, though the signal processing is

* Corresponding author. E-mail address: iradiratu@hangtuah.ac.id
Tel.: +62 857-5525-5203; Fax: +031 5946261

conducted by acquisition, de-noising, pre-fault component cancellation, and feature extraction [11]. In contrast, non-invasive techniques include the diagnosis of thermal, vibration, and sound damage. Thermal data diagnosis requires the expensive fiber Bragg grating (FBG) sensor, and it is further developed by processing the data through images, which requires several complicated stages. The image obtained from the camera capture is processed to diagnose motor conditions [12]. Diagnosis through vibration is applied only by using a piezoelectric accelerometer. However, the results are susceptible to the engine body friction with the pedestal and different engine casing problems [13].

Data obtained invasively or non-invasively are processed using certain algorithms recommended for fault diagnosis. These algorithms include wavelet transform, fast Fourier transform (FFT), Hilbert transform, park vector analysis, and machine learning [14]. The wavelet transform is a signal processing algorithm that determines the motor condition. However, it cannot identify the faulty part, damage to the bearings, rotor, stator, or eccentricity because the Wavelet algorithm undergoes decomposition in its analysis [15]. Park vector analysis compares the vector's shape and thickness, where round and elliptical patterns indicate a healthy and damaged motor, respectively [16]. The widely used signal processing algorithm is FFT because of its high success rate [17]. The FFT signal determines the condition of the engine parts by comparing the damage frequency amplitude. Therefore, studies on motor condition monitoring recommended diagnostic techniques through FFT sound signals and processing [2].

The recommended non-invasive technique is damage diagnosis through sound because it is easy, inexpensive, and applicable to all motor parts [18]. Although the technique monitors the engine's condition using sound signals, it performs poorly because the engine sound signal easily overlaps with others. Occasionally, the sound signal does not change with the engine process. Digital signal processing applications for machine monitoring require input signals and certain methods. The data from the sensor is processed through a signal with FFT and filtered to obtain the correct engine condition diagnosis [19]. Comparing the sound signal processing with the Hilbert–Huang and the FFT algorithms show that the FFT algorithm is more effective for bearing damage detection [20]. Damage detection using sound signal data with a band-pass filter contributes to the detection results' accuracy [21]. This means fault detection through sound signal is recommended for detecting machine parts with higher accuracy

The purpose of this study is developing analytical methodologies for detecting damage to induction motors operating at various loads and the degree of damage to outer race bearings on the main and fan shaft rotors. Despite the high accuracy, some studies showed that it is not specific to check whether the diagnosed bearing is located on the main or fan shaft. This is because damaged bearing conditions with different locations on the shaft affect the motor's sound characteristics. Therefore, this study applied a non-invasive diagnostic technique by detecting damage to the bearing's outer race. An induction motor sound analysis was conducted by considering the damaged bearing's location on the shaft. Bearings in induction motors are located on the main and fan shafts. Damage to the fan shaft bearings is rougher or harder than the main shaft. Furthermore, the bearing damage alters the motor's sound characteristics.

Previous studies conducted tests by providing a hole defect in the bearing [1, 5, 7-8]. The results show that the damage detection system could identify the bearing conditions, however, the research did not test the minor damage. This study tested the outer race-bearing cracks and minor damage that cause other defects. To observe the occurring harmonics, it used the FFT algorithm to calculate the outer-race breakdown frequency. The bearing was declared faulty using eight harmonic components when the sound harmonic component exceeded that of a healthy motor and vice versa. This conclusion is a reference for detecting damage to the outer race bearing useful information on maintenance actions before serious damage occurs.

Section 2 of this study describes the configuration of the damage detection system used, while section 3 reviews the object of diagnosis, signal processing, and filtering to determine the frequency of fault locations. Additionally, section 4 discusses the experiment results, while section 5 presents conclusions.

2. System Configuration

This study applied damage detection to a three-phase motor with a squirrel cage rotor type of 1.5 kW. The damage detection system through sound signals requires supporting equipment, including a 3-phase power supply, mechanical braking, sound sensors, and signal processing MATLAB software. The sound sensor uses a microphone placed 10 cm from the motor body. The distance should be considered to obtain data not influenced by the motor fan sound and non-machine noise. Therefore, the sound data was processed with the FFT algorithm to obtain a sound spectrum graph showing the harmonics of the outer race bearing damage frequency. Fig. 1 shows a detection system that identifies the condition of the outer race bearing through a sound signal. This study tested the placement of damaged outer race bearings on different shafts, the level of damage, and loading variations. The motor under load conditions was tested by providing mechanical loading with the main shaft rotor connected to the clutch and lever to provide a braking effect. The test showed that adding a load on the detection system changes the sound spectrum characteristics. The load variations included Loads 1, 2, 3, and 4 as 0, 30, 40, and 50 Newtons, respectively.

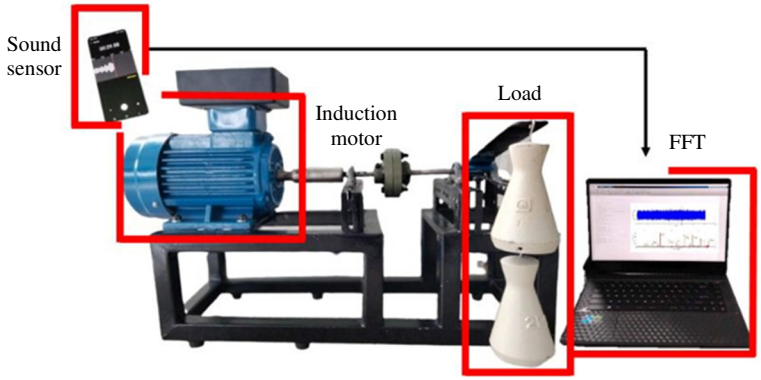

Fig. 1 Damage detection system configuration

3. Bearing and Frequency of Damage

Bearings comprise the inner race, ball, cage, and outer race bearings, all of which function as components helping the motor move freely. Table 1 shows the specifications of the bearings used as test specimens, while Fig. 2 shows the bearing position on the rotor shaft and the induction motor construction. Bearing damage starts minor before progressing severe and results from incorrect installation, lack of lubricant, overload, and brinelling.

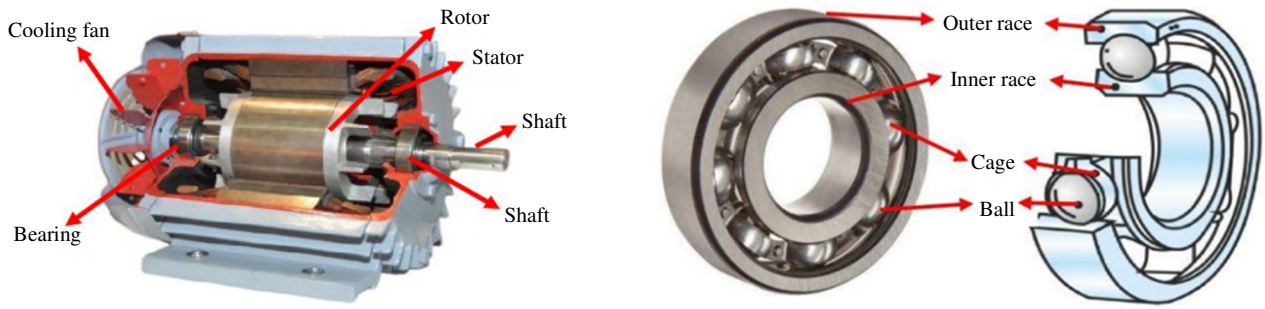

(a) Induction motor construction (b) Bearing construction

Fig. 2 Induction motor and bearing construction

This study performed tests by reconstructing the outer race bearing, as shown in Fig. 3. The three cases of damage to the outer race bearing were Fault#1 (cracked), Fault#2 (1 mm diameter hole), and Fault#3 (2 mm diameter hole). Damage may occur to bearings on the fan or main shaft. When both shaft parts are damaged, an imbalance in the rotor's rotation will occur. Variations in motor loading, faulty bearing locations on the rotor shaft, and damage levels change the motor's speed, sound, and sound signal spectrum characteristics. Therefore, it is necessary to calculate the damage frequency characteristics for diagnosis.

Fig. 3 Outer race bearing damage

Changes in the rotor's rotational speed affect the damage frequency characteristics used to identify the condition of each bearing element. Eqs. (1)-(4) predict the damage frequency based on the diagnosis location of the bearing section [8]. N_b is the number of ball bearings, nm is the rotational speed, B_d is the diameter of the ball, D is the pitch diameter, and α is the ball's contact angle

$$\text{Outer-race bearing: } f_o = \frac{N_b}{2} nm\left(1-\frac{B_d}{D}\cos\alpha\right) \tag{1}$$

$$\text{Inner-race bearing: } f_i = \frac{N_b}{2} nm\left(1+\frac{B_d}{D}\cos\alpha\right) \tag{2}$$

$$\text{Ball bearing: } f_{ball} = \frac{N_b}{2D} nm\left[1-\left(\frac{B_d}{D}\cos\alpha\right)^2\right] \tag{3}$$

$$\text{Cage bearing: } f_{cage} = \frac{1}{2} nm\left(1-\frac{B_d}{D}\cos\alpha\right) \tag{4}$$

Harmonic component's damage frequency predictions were repeated with an increasing constant value, as shown in Eq. (5), f_p is the predicted fault frequency, f_v is the fault characteristic frequency obtained from Eqs. (1)-(4), and k is a constant $k = 1, 2, 3, \cdots$.

$$f_p = |k.f_v| \tag{5}$$

Calculating the damage characteristic frequency before a diagnosis facilitates observation. Table 1 shows the bearing specifications used in this study.

Table 1 Bearing specification

Brand	CSC
Type	6205 2R
Inside diameter (Inner)	25 mm
Number of balls	9 pieces
Ball bearing diameter	7.25 mm
Outside diameter (Outer)	52 mm

The following is an example calculation of the frequency of damage to outer race bearing Fault#2, with load 1 using Eq. (1), with parameters $N_b = 9$, $B_d = 7.25\ mm$, contact angle $\alpha = 0$ so $\cos\alpha = 1$, and a speed of 1495.7 (tachometer measurement): $nm = \frac{1495.7}{60} = 24.92\ rev/sec$, $D = \frac{52+25}{2} = 38.5$, and $f_0 = \frac{9}{2}24.92\left(1-\frac{7.25}{38.5}\cos 0^\circ\right) = 91.05$ Hz

Table 2 shows the calculation results on the damage frequency characteristics with several load and damage level variations. The damage characteristic frequency was used to determine the damage frequency's harmonic component. Eight harmonic components were observed, meaning the selected constant k is up to $k = 8$. Detailed and valid detection results are obtained by observing more harmonic components

Table 2 Outer race bearing damage frequency

Load	Condition bearing		
	Fault#1 (Hz)	Fault#2 (Hz)	Fault#3 (Hz)
0 Newton (load1)	94.99	91.05	91.35
30 Newton (load2)	93.97	91.51	90.99
40 Newton (load3)	94.05	91.56	91.56
50 Newton (load4)	94.67	91.64	91.56

4. Results and Discussion

The damage frequency calculation was used to diagnose damage to the outer race bearing. This study discussed the characteristics of the sound signal from damaged bearing conditions with different locations, loading variations, and damage levels. Outer race bearing damage was tested on the fan and main shaft rotor. The motor's condition was identified based on the signal from two outer race-bearing conditions. This implies the sound signal of a healthy motor condition is a reference and a test signal. Furthermore, motor sound diagnostic data were collected by observing the effect of ambient noise in the room. Noise from other than motors greatly affects the analysis results. Therefore, to obtain valid data, preprocessing which involves studying the ambient sound and its effect on the detection results is necessary. Tests were conducted in quiet, standard, and crowded conditions to determine the effect of noise on the damage detection results. The quiet and standard room conditions from the reprocessing stage allow sound recording as the main data to detect outer-race conditions.

4.1. Sound signal time-domain analysis

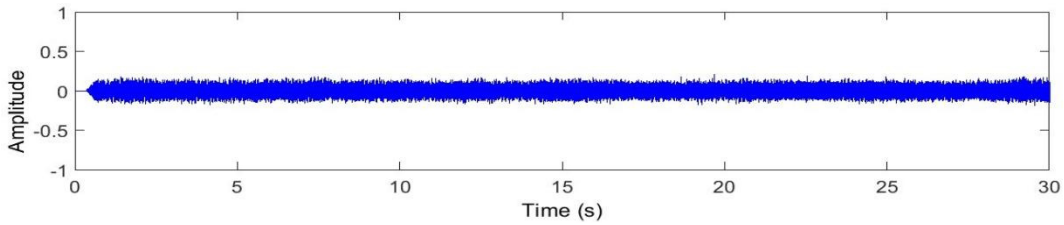

Fig. 4 Motor sound signal in healthy condition

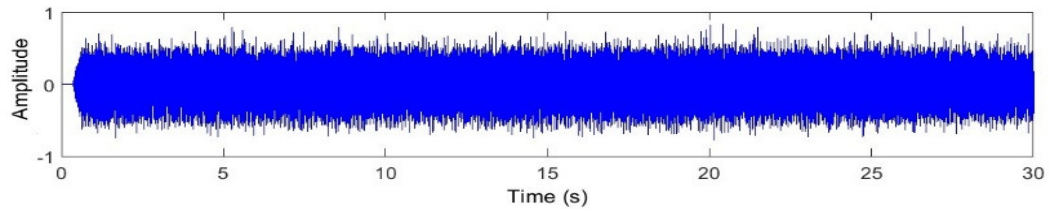

Fig. 5 The sound signal of the motor in the outer race bearing is damaged and placed on the fan shaft

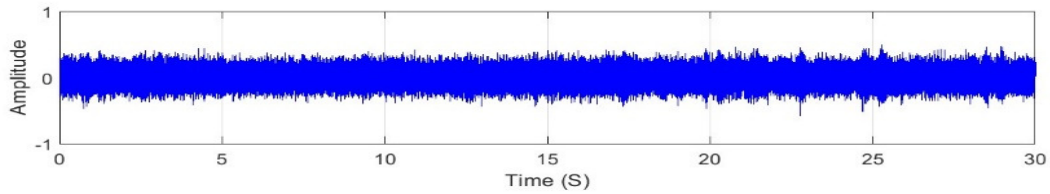

Fig. 6 The sound signal of the motor is that the outer race bearing is damaged and placed on the main shaft

Figs. 4-6 present the time-domain sound signals for healthy motors and faulty outer race bearings. The sound signal was obtained from the microphone at 44.1KHz, an average recording of 30 seconds, and placed 10 cm from the motor body. Fig. 4 is a sound signal for a healthy outer race bearing, where the average amplitude is around 0.18, while Figs. 5-6 show the increase in mean amplitude. An increase in the motor sound signal amplitudes indicates an abnormality in the motor part (Fault#2). In Fig. 5, the sound signal from the damaged outer race bearing on the fan shaft has greater amplitude, with an average of 0.6.

When the outer race bearing is damaged, it is placed on the main shaft with an average of 0.3 and makes a louder sound when placed on the fan shaft. The differences in sound characteristics should be discussed to assess their effect on damage detection. Therefore, this study conducted further sound signal processing to determine whether the sound characteristics had a validity effect on damage detection. Analyzing sound characteristics in the time domain cannot determine the location of the damaged motor part. This necessitates FFT to transform the sound signal from the time to the frequency domain.

4.2. Sound signal frequency domain analysis

The motor parts' condition is determined by observing the frequency amplitude when the damage occurs. The calculation results in Table 2 imply the necessity to observe the amplitude of each harmonic at the damage frequency. Fig. 7 shows the resulting FFT transformation spectrum for a healthy motor. The eight harmonic components were displayed at the fault location frequency. Furthermore, the healthy motor condition's amplitude helps determine the motor's condition. Some reference frequency points include 91.05 Hz, 182.1 Hz, 273.2 Hz, 364.2 Hz, 455.3 Hz, 546.3 Hz, 637.4 Hz, and 728.4 Hz. Fig. 7 shows several dominant frequencies, including 100Hz, 300Hz, and 650Hz. However, they are not used for fault diagnosis because they are not harmonic components of the outer - race bearing fault frequency. The outer race bearing was tested in a damaged condition after obtaining the amplitude of the harmonic components in a healthy outer race. The damage to the motor parts started with minor damage, and it could lead to severe damage.

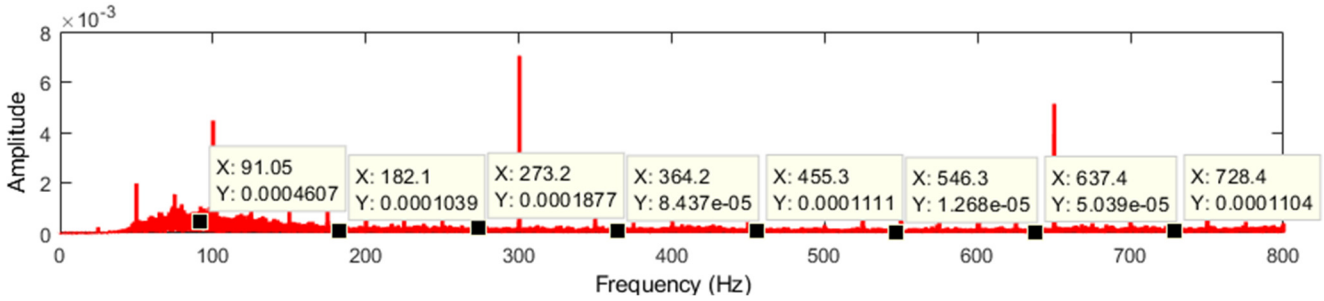

Fig. 7 The sound spectrum of a healthy motor used as a reference

The results appropriate to the damage were obtained by conducting detection tests on the outer race bearing when cracked (Fault#1) and under other severe damage (Fault#2 and Fault#3). The test involved alternating the damaged bearing on the fan or main shaft. Damaged bearings are not placed on both shaft parts because they will result in motor eccentricity, causing a separate frequency outside the bearing damage frequency. Fig. 8 shows the sound spectrum on a faulty bearing test on a fan shaft with load 1, where (a) is Fault#1, (b) Fault#2, and (c) Fault#3. The amplitude of each harmonic component in the breakdown frequency was observed. A test amplitude exceeding the healthy value means the outer race is damaged and the actual condition could be detected. In contrast, a test amplitude not exceeding the healthy values indicates that the outer race is healthy, and the table is gray. This means the system does not recognize the outer race bearing's actual condition, implying false detection.

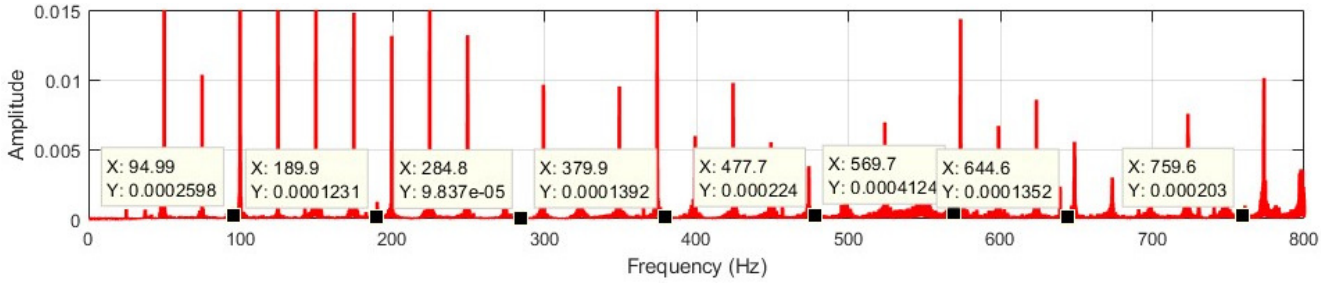

(a) Sound spectrum on Fault#1 Load1 test

Fig. 8 The sound spectrum of the damaged outer race bearing is located on the fan shaft rotor with the load1 case

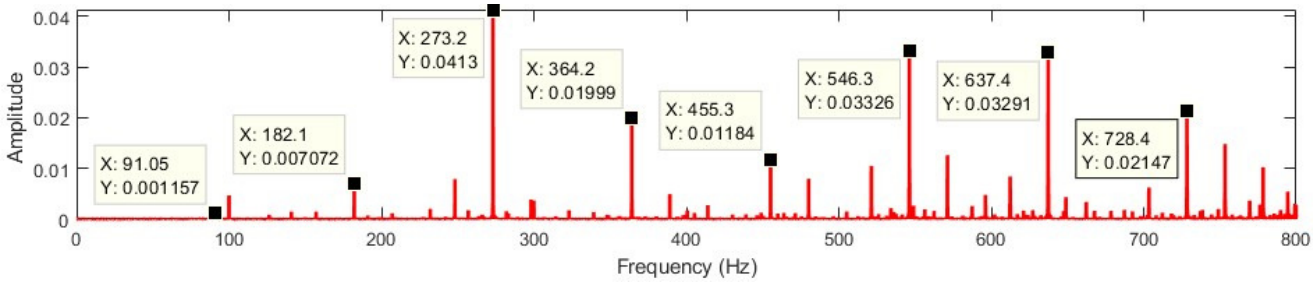

(b) Sound spectrum on Fault#2 Load1 test

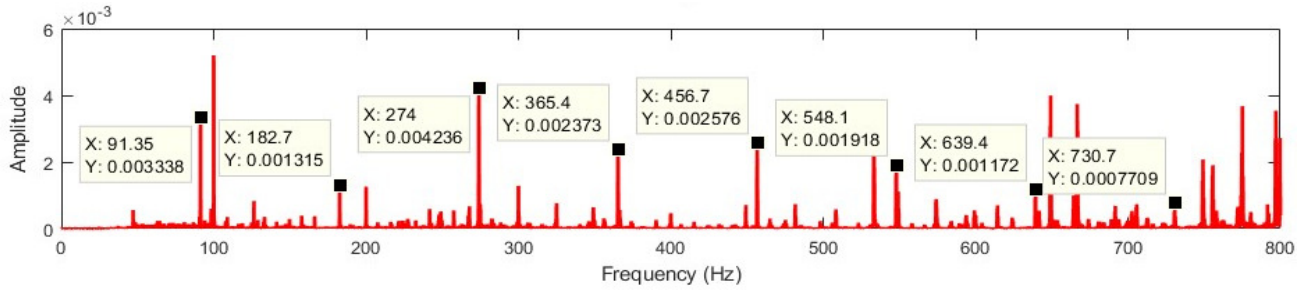

(c) Sound spectrum on Fault#3 Load1 test

Fig. 8 The sound spectrum of the damaged outer race bearing is located on the fan shaft rotor with the load1 case (continued)

The amplitude for each outer race bearing frequency harmonics from Fig. 8 are shown in Table 3. These values facilitate comparing the test amplitude with the reference amplitude. The left column in Table 3 shows that the test on the outer race-bearing crack (Fault#1) has two undetectable frequency points of harmonic damage. The f_o and f_{ox3} harmonics have a smaller amplitude than the reference amplitude, greatly affecting the detection accuracy by 75%. The rough sound character caused by minor damage on the outer race bearing on the fan shaft also affects the detection accuracy. However, the amplitude exceeds the healthy value in tests with damage levels of Fault#2 and Fault#3, when the calculated detection accuracy percentage would be 100%. These results show that the detection system developed has recognized the outer-race bearing condition with high accuracy in testing the holes in the fan shaft rotor.

Table 3 Fault#1, Fault#2, and Fault#3 outer race bearing damage detection analysis when placed on the fan or main shaft

Frequency	Healthy condition	Amplitude test outer race bearing damaged condition in the fan shaft rotor			Amplitude test outer race bearing damaged condition in the main rotor		
		Fault#1	Fault#2	Fault#3	Fault#1	Fault#2	Fault#3
f_o	0.00046	0.00025	0.00115	0.00333	0.00080	0.00118	0.00106
f_{ox2}	0.00010	0.00012	0.00707	0.00131	0.00120	0.00042	0.00108
f_{ox3}	0.00018	0.00009	0.04130	0.00423	0.00035	0.00054	0.00404
f_{ox4}	0.00008	0.00013	0.01999	0.00237	0.00007	0.00012	0.00087
f_{ox5}	0.00011	0.00022	0.01184	0.00257	0.00030	0.00024	0.00014
f_{ox6}	0.00001	0.00041	0.03326	0.00191	0.00065	0.00394	0.00396
f_{ox7}	0.00005	0.00013	0.03291	0.00117	0.00016	0.00062	0.00299
f_{ox8}	0.00011	0.00020	0.02147	0.00077	0.00017	0.00100	0.01426
Broken detected		6	8	8	8	8	8
% detection accuracy		75%	100%	100%	100%	100%	100%

The detection results were confirmed by testing the damaged outer race bearing on the main shaft rotor. Fig. 9 presents the sound spectrum on the test of a faulty outer race bearing on the main shaft with variations of Fault#1, Fault#2, and Fault#3. The test amplitudes for damaged outer race bearings on the main shaft are presented in the right column of Table 3. All harmonic frequencies detect the actual condition of the outer race bearing. Placing the outer race bearing, broken conditions, cracks, and other damage to the main shaft did not affect the accuracy of the detection results, meaning the percentage of detection accuracy is 100%.

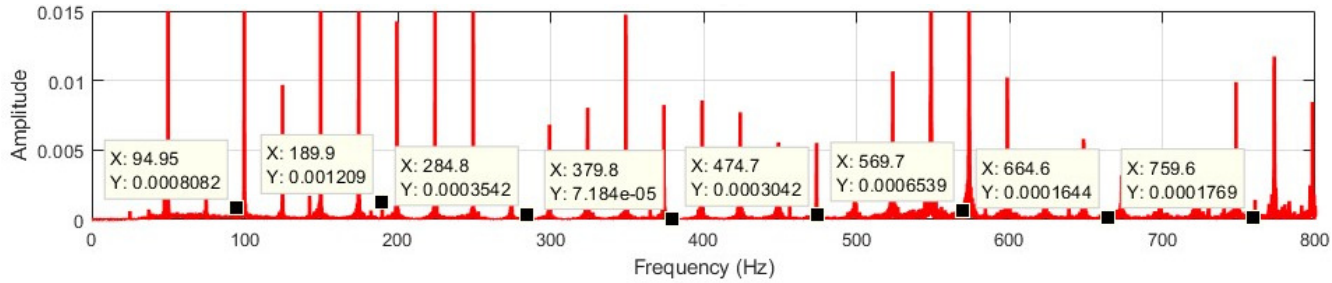

(a) Sound spectrum on Fault#1 Load1 test

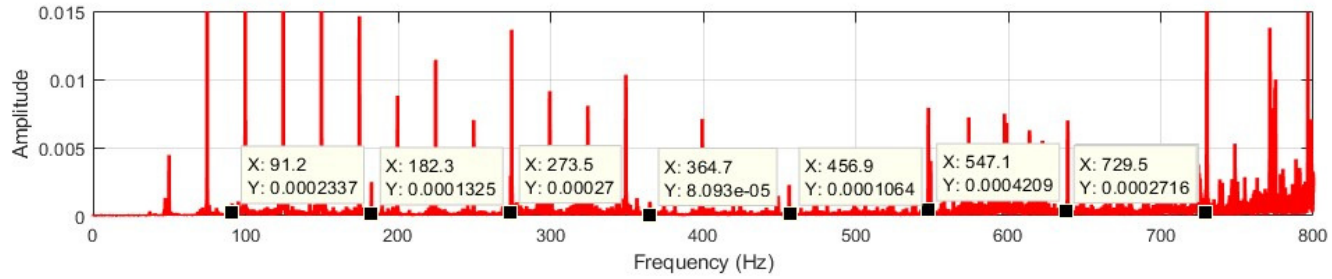

(b) Sound spectrum on Fault#2 Load1 test

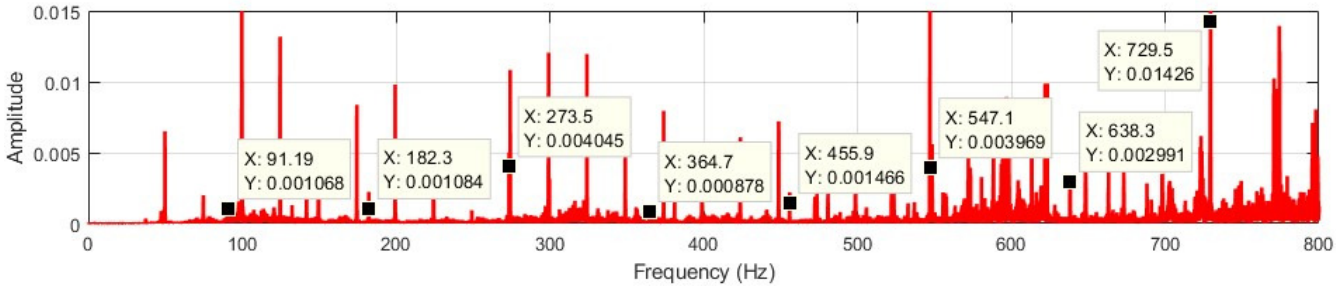

(c) Sound spectrum on Fault#3 Load1 test

Fig. 9 The sound spectrum of the damaged outer race bearing is located on the main shaft rotor with a load1 case

The analysis was conducted under different load conditions because the induction motor operates with load variations. The outer race bearing was placed on the fan shaft rotor in a damaged condition, and the decrease in detection accuracy was considered for further testing. The sound spectrum and analysis in the load 2 case are shown in Fig. 10 and Table 4 in the left column. In Fig. 10, the spectrum graph shows several dominant frequencies, including 50 Hz, 100 Hz, and 150 Hz. The three dominant frequencies were not observed for damage analysis because they do not show the outer race-bearing damage frequency. Furthermore, the graph of the test spectrum for loads with Fault#2 case shows that all harmonic frequencies detect outer race bearing damage. The highest dominant damage frequency of 0.02908 was obtained at the 6th harmonic. Other harmonic frequencies are not lower than the reference amplitude, implying 100% detection accuracy. Moreover, testing case load#3 and load#2 shows that the harmonic frequency of damage f_o is healthy. This means the detection system does not recognize damage to the outer race bearing, implying a damage detection accuracy of 87.5%, while other frequencies indicate damage.

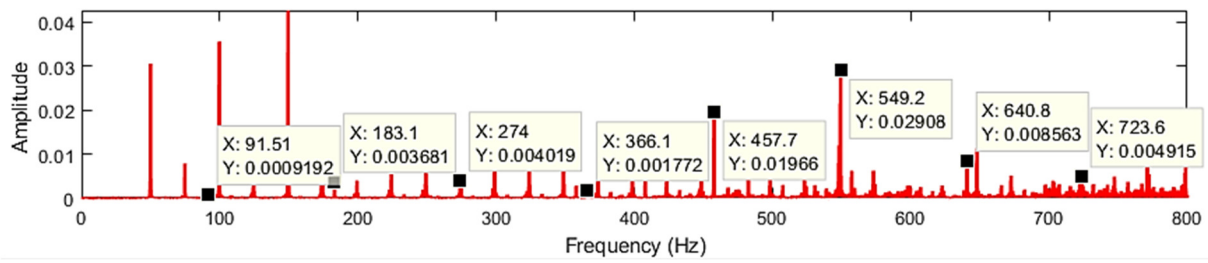

(a) Sound spectrum Fault#2 case

Fig. 10 Sound spectrum load2 variation testing

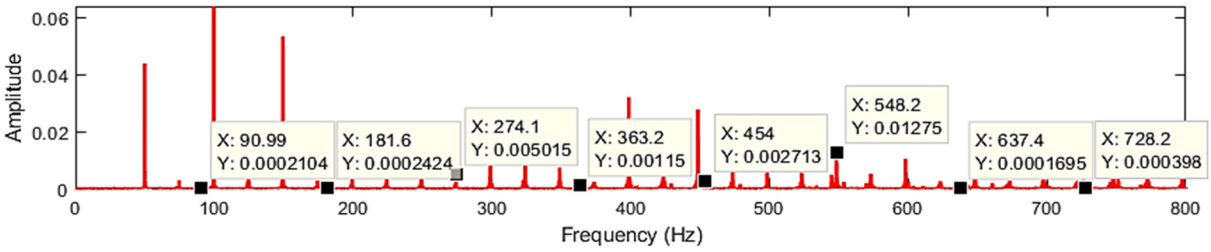

(b) Sound spectrum Fault#3 case

Fig. 10 Sound spectrum load2 variation testing (continued)

Loads 3 and 4 tests involved observing the amplitude in each damage harmonic spectrum, and the results are presented in the middle and right columns of Table 4. The shading sign means the damage harmonic frequency point indicates a healthy outer race condition, implying an incorrect test because the race being tested is damaged. Additionally, the results on the variation of load3 show that Fault#2 at f_{ox3} and Fault#3 at f_o do not detect damage. The percentage of accuracy obtained is 87.5% because one frequency point does not detect damage. Tests on variations in load 4 show that all damage frequencies detect damage, indicating 100% detection accuracy.

Table 4 Damage detection results for all load variations

Frequency	Load2 testing amplitude			Load3 testing amplitude			Load4 testing amplitude		
	Healthy	Fault#2	Fault#3	Healthy	Fault#2	Fault#3	Healthy	Fault#2	Fault#3
f_o	0.00035	0.00091	0.00021	0.00032	0.00312	0.00020	0.00002	0.00053	0.00030
f_{ox2}	0.00020	0.00368	0.00024	0.00017	0.00296	0.00022	0.00002	0.00283	0.00029
f_{ox3}	0.00474	0.00401	0.00501	0.00207	0.00131	0.00327	0.000002	0.00451	0.00517
f_{ox4}	0.00036	0.00177	0.00115	0.00008	0.00151	0.00197	0.00005	0.00150	0.00163
f_{ox5}	0.00046	0.01966	0.00271	0.00007	0.01234	0.00017	0.00002	0.01719	0.00392
f_{ox6}	0.00019	0.02908	0.01275	0.00044	0.01304	0.00113	0.00003	0.02171	0.00765
f_{ox7}	0.00014	0.00856	0.00016	0.00004	0.00589	0.00025	0.00001	0.00614	0.00029
f_{ox8}	0.000008	0.00491	0.00039	0.00011	0.00500	0.00067	0.00015	0.00313	0.00487
Damage detected		8	7		7	7		8	8
% detection accuracy		100%	87.5%		87.5%	87.5%		100%	100%

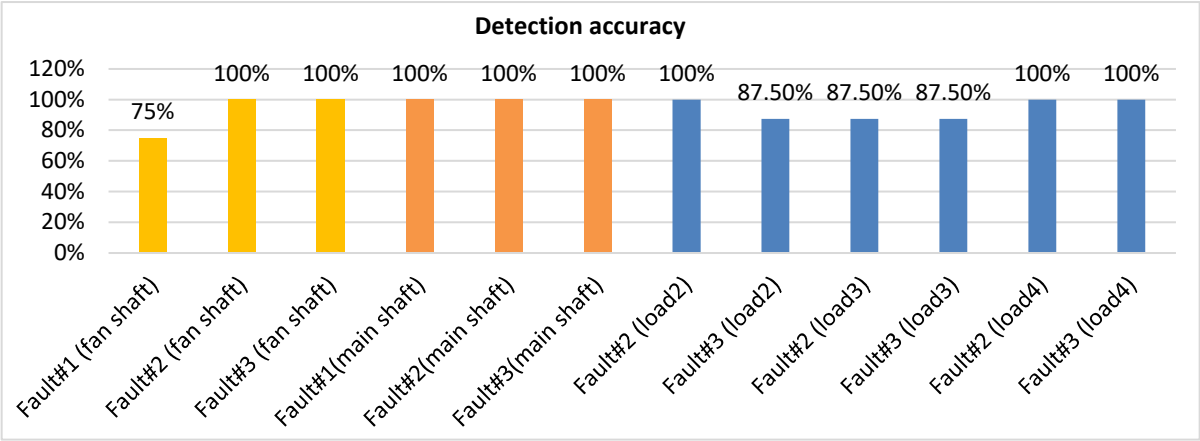

Fig. 11 Summarizes the percentage accuracy of damage detection

Fig. 11 summarizes the percentage accuracy of damage detection in all tests. The effect of damaged outer race bearings on the fan and main shafts is 91.66% and 100%, respectively. The average of testing on loading variations is 93.75%, meaning that the detection using sound has high accuracy. Preprocessing was needed to obtain sound data free from non-machine noise, which strongly influences damage detection. Additionally, damage detection through sound is the recommended technique supported by the advantages of non-invasive methods. Table 5 shows previous studies on bearing damage detection using

sound signals. It shows the use of multiple sensors, testing with load variations, testing the damage to bearings on different rotor shafts, and presenting accurate results. Furthermore, the proposed method gets good accuracy. [21] did not include the accuracy obtained but tested all bearing and other motor parts, which could be an input for testing in further studies. Moreover, the proposed method provides an accuracy that should be considered because the test provides variations in loading, damage levels, and damaged bearing conditions in different locations. Determining the diagnosis frequency appropriate with the damage location could help the diagnosis observation with a 93.75% accuracy.

Table 5 Comparison of the accuracy of similar studies

Study	Using more than one sensor	Load variation test	Testing of variations in the damage to the outer race	Testing for variations in the location of damaged bearings on the shaft	Accuracy percentage
Hecke et al., 2015 [21]	No	No	No	No	-
Junior et al., 2020 [22]	No	No	Yes	No	100%
Lu et al., 2019 [23]	Yes	No	No	No	87%
Proposed method	No	Yes	Yes	Yes	93.75%

5. Conclusions

This study discussed damage analysis using sound signals with processing algorithms using FFT. The amplitude ratio to the damage frequency determines the outer race-bearing condition. Moreover, the damage location, level, and load variation significantly affect the motor condition diagnosis. The frequency should be calculated under different test conditions, as the finding showed a decrease in accuracy when the damaged bearing is placed on the fan shaft rotor. This is because the test was performed on cracked bearings, reducing the effect of the sound spectrum amplitude. Sound data retrieval is strongly influenced by a fan motor and non-engine noise, causing diagnosis errors. This is avoided by preprocessing data retrieval by determining the right distance. Furthermore, a minimum distance of 10 cm is taken because the fan noise on the shaft affects the diagnosis when the microphone is closer.

(1) The detection system is 91.66% and 100% accurate when testing the damaged bearing on the fan and main shaft rotors, respectively. Similarly, the time-domain sound analysis shows a smoother sound than bearing damage on the fan shaft rotor. This reveals that the damage level and the bearing's damage location on the shaft slightly affect the accuracy of bearing condition detection.

(2) Load variation changes the motor’s sound, with a high percentage of 93.75% for the proposed detection accuracy test. Damage detection through sound using FFT is recommended to identify the induction motor’s condition, though the data is affected by the non-engine and fan noise on the rotor shaft.

(3) The motor’s sound has a wide frequency range, but the damage location frequency should be calculated based on the location observed. This filtering step or band-pass determines the location of the amplitude observations as a diagnosis of the outer-race bearing condition.

Moreover, the filter results’ prediction frequency promises are more accurate by observing the amplitude at the fault location in the harmonic components. The proposed method could diagnose the condition of other motor parts, including bearing parts, rotor bars, stators, and eccentricity. However, the speed changes affect the damage frequency location determination, requiring accuracy and necessitating observing the rotation value at each diagnosis.

Acknowledgments

The authors thank the Electrical Machinery Laboratory of Hang Tuah University for the insights and expertise in conducting this study. They also thank the study team of the Energy Conversion Laboratory, Hang Tuah University, for their comments and suggestions for manuscript improvement.

Conflicts of Interest

The authors declare there is no conflict of interest.

References

[1] I. D. PK, B. Y. Dewantara, and W. M. Utomo, "Healthy Monitoring and Fault Detection Outer Race Bearing in Induction Motor Using Stator Current," International Journal of Integrated Engineering, vol. 11, no. 3, pp. 181-193, September 2019.

[2] A. Abdo, J. Siam, A. Abdou, R. Mustafa, and H. Shehadeh, "Electrical Fault Detection in Three-Phase Induction Motor Based on Acoustics," IEEE International Conference on Environment and Electrical Engineering and IEEE Industrial and Commercial Power Systems Europe, pp. 1-5, June 2020.

[3] A. Daraz, S. Alabied, A. Smith, F. Gu, and A. D. Ball, "Detection and Diagnosis of Centrifugal Pump Bearing Faults Based on the Envelope Analysis of Airborne Sound Signals," International Conference on Automation and Computing, pp. 1-6, September 2018.

[4] M. Irfan, N. Saad, R. Ibrahim, V. S. Asirvadam, A. S. Alwadie, and M. A. Sheikh, https://www.intechopen.com/chapters/54865, May 31, 2017.

[5] D. P. Iradiratu, B. Y. Dewantara, D. Rahmatullah, I. Winarno, and C. Hidayanto, "Decomposition Wavelet Transform as Identification of Outer Race Bearing Damage through Stator Flow Analysis in Induction Motor," International Conference on Information and Communications Technology, pp. 733-737, July 2019.

[6] A. Choudhary, T. Mian, and S. Fatima, "Convolutional Neural Network Based Bearing Fault Diagnosis of Rotating Machine Using Thermal Images," Measurement, vol. 176, Article no. 109196, May 2021.

[7] X. Song, Z. Wang, and J. Hu, "Detection of Bearing Outer Race Fault in Induction Motors Using Motor Current Signature Analysis," 22nd Internation Conference on Electrical Machines and Systems, pp.1-5, August 2019.

[8] M. R. Barusu and M. Deivasigamani, "Non-Invasive Vibration Measurement for Diagnosis of Bearing Faults in 3-Phase Squirrel Cage Induction Motor Using Microwave Sensor," IEEE Sensors Journal, vol. 21, no. 2, pp. 1026-1039, January 2021.

[9] M. Zuhaib, F. A. Shaikh, U. A. Shaikh, and A. Soomro, "An Approach on MCSA-Based Fault Detection Using Discrete Wavelet Transform and Fault Classification Based on Deep Neural Networks," International Journal of Advanced Trends in Computer Science and Engineering, vol. 10, no. 3, pp. 2256-2259, June 2021.

[10] V. Becker, T. Schwamm, S. Urschel, and J. Antonino-Daviu, "Fault Detection of Circulation Pumps on the Basis of Motor Current Evaluation," IEEE Transactions on Industry Applications, vol. 57, no. 5, pp. 4617-4624, June 2021.

[11] K. D. Kompella, N. S. Rongala, S. R. Rayapudi, and V. G. R. Mannam, "Robustification of Fault Detection Algorithm in a Three-Phase Induction Motor Using MCSA for Various Single and Multiple Faults," IET Electric Power Applications, vol. 15, no. 5, pp. 593-615, November 2021.

[12] A. Mohammed and S. Djurović, "Electric Machine Bearing Health Monitoring and Ball Fault Detection by Simultaneous Thermo Mechanical Fibre Optic Sensing," IEEE Transactions on Energy Conversion, vol. 36, no. 1, pp. 71-80, June 2020.

[13] T. Amanuel, A. Ghirmay, H. Ghebremeskel, R. Ghebrehiwet, and W. Bahlibi, "Design of Vibration Frequency Method with Fine-Tuned Factor for Fault Detection of Three Phase Induction Motor," Journal of Innovative Image Processing, vol. 3, no. 1, pp. 52-65, April 2021.

[14] P. Kumar and A. S. Hati, "Review on Machine Learning Algorithm Based Fault Detection in Induction Motors," Archives of Computational Methods in Engineering, vol. 28, no. 3, pp. 1929-1940, June 2021.

[15] M. A. Hmida and A. Braham, "Fault Detection of VFD-Fed Induction Motor under Transient Conditions Using Harmonic Wavelet Transform," IEEE Transactions on Instrumentation and Measurement, vol. 69, no. 10, pp. 8207-8215, May 2020.

[16] F. Husari and J. Seshadrinath, "Inter-Turn Fault Diagnosis of Induction Motor Fed by PCC-VSI Using Park Vector Approach," IEEE International Conference on Power Electronics, Drives, and Energy Systems, pp. 1-6, December 2020.

[17] M. Jalayer, C. Orsenigo, and C. Vercellis, "Fault Detection and Diagnosis for Rotating Machinery: A Model Based on Convolutional LSTM, Fast Fourier and Continuous Wavelet Transforms," Computers in Industry, vol. 125, article no. 103378, December 2021.

[18] O. AlShorman, F. Alkahatni, M. Masadeh, M. Irfan, A. Glowacz, F. Althobiani, et al., "Sounds and Acoustic Emission-Based Early Fault Diagnosis of Induction Motor: A Review Study," Advances in Mechanical Engineering, vol. 13, no. 2, pp. 1-19, February 2021.

[19] D. Goyal, C. Mongia, and S. Sehgal, "Applications of Digital Signal Processing in Monitoring Machining Processes and Rotary Components: A Review," IEEE Sensors Journal, vol. 21, no. 7, pp. 8780-8804, April 2021.

[20] V. K. Rai and A. R. Mohanty, "Bearing Fault Diagnosis Using FFT of Intrinsic Mode Functions in Hilbert-Huang Transform," Mechanical Systems and Signal Processing, vol. 21, no. 6, pp. 2607-2615, August 2007.

[21] B. Van Hecke, Y. Qu, and D. He, "Bearing Fault Diagnosis Based on a New Acoustic Emission Sensor Technique," Proceedings of the Institution of Mechanical Engineers, Part O: Journal of Risk and Reliability, vol. 229, no. 2, pp. 105-118, November 2015.

[22] J. A. Lucena-Junior, T. L. de Vasconcelos Lima, G. P. Bruno, A. V. Brito, J. G. G. de Souza Ramos, F. A. Belo, et al., "Chaos Theory Using Density of Maxima Applied to the Diagnosis of Three Phase Induction Motor Bearings Failure by Sound Analysis," Computers in Industry, vol. 123, article no. 103304, December 2020.

[23] S. Lu, P. Zheng, Y. Liu, Z. Cao, H. Yang, and Q. Wang, "Sound-Aided Vibration Weak Signal Enhancement for Bearing Fault Detection by Using Adaptive Stochastic Resonance," Journal of Sound and Vibration, vol. 449, pp. 18-29, June 2019.